

DeepVRegulome: DNABERT-based deep-learning framework for predicting the functional impact of short genomic variants on the human regulome

Pratik Dutta,^{1*} Matthew Obusan², Rekha Sathian¹, Max Chao¹, Pallavi Surana¹, Nimisha Papineni¹, Yanrong Ji³, Zhihan Zhou⁴, Han Liu⁴, Alisa Yurovsky¹, and Ramana V Davuluri^{1*}

¹Department of Biomedical Informatics, Stony Brook University, Stony Brook, NY, ²Renaissance School of Medicine, Stony Brook University, Stony Brook, NY, ³Division of Health and Biomedical Informatics, Department of Preventive Medicine, Northwestern University Feinberg School of Medicine, ⁴Department of Computer Science, Northwestern University, Evanston, IL, USA.

Abstract

Whole-genome sequencing (WGS) has revealed numerous non-coding short variants whose functional impacts remain poorly understood. Despite recent advances in deep-learning genomic approaches, accurately predicting and prioritizing clinically relevant mutations in gene regulatory regions remains a major challenge. Here we introduce **DeepVRegulome**, a deep-learning method for prediction and interpretation of functionally disruptive variants in the human regulome, which combines 700 DNABERT fine-tuned models, trained on vast amounts of ENCODE gene regulatory regions, with variant scoring, motif analysis, attention-based visualization, and survival analysis. We showcase its application on TCGA glioblastoma WGS dataset in prioritizing survival-associated mutations and regulatory regions. The analysis identified 572 splice-disrupting and 9,837 transcription-factor binding site altering mutations occurring in greater than 10% of glioblastoma samples. Survival analysis linked 1352 mutations and 563 disrupted regulatory regions to patient outcomes, enabling stratification via non-coding mutation signatures. All the code, fine-tuned models, and an interactive data portal are publicly available.

Introduction

Whole genome sequencing (WGS)^{1,2} data across large cancer cohorts provide a comprehensive catalogue of mutations, which include short variants, such as single nucleotide variants (SNVs) and small insertions and deletions (indels)³⁻⁵. While advances in variant calling have improved detection of somatic mutations, interpreting their functional impact—particularly in non-coding regions—remains a major challenge^{6,7}. These non-coding mutations can affect splice sites, promoters, enhancers, and transcription-factor binding sites (TFBSs), thereby modulating gene expression and activity without altering protein structures^{8,9}. For instance, mutations in TFBS may disrupt transcription-factor binding, leading to aberrant gene expression⁸, while alterations in splice sites may result in alternative splicing^{10,11}, generating dysfunctional protein isoforms^{12,13}. The need for sophisticated computational models to interpret non-coding mutations is, therefore, paramount, as conventional annotation methods are not sufficient for these complex regulatory sequences^{14,15}.

Recent advancements in deep learning methods have introduced models yielding promising results across biological applications, such as gene expression prediction¹⁶, drug discovery¹⁷, protein function analysis^{18,19}, disease prognosis^{20,21}, and non-coding variant effect prediction⁹. Specialized models for non-coding variant analysis include ARVIN²², which identifies non-coding risk variants in promoters and enhancers, Basenji²³, which annotates mutations with chromatin accessibility changes, DeepBind²⁴, predicting DNA/RNA-binding protein affinities, and DeepSEA²⁵, which assesses genomic variant effects on transcription factor binding, DNase I hypersensitive sites, and histone marks. These models address different aspects of gene regulation, offering powerful tools for variant impact analysis. Concurrently, large language models (LLMs) such as BigBird²⁶ and DNABERT²⁷ leverage transformer architectures with k-mer tokenization to capture genomic sequence context, aiding in tasks like masked language modeling (MLM). Extensions of this paradigm include epigenome-aware transformers (GeneBERT²⁸, Epigenomic-BERT²⁹) that incorporate chromatin signals, long-context models (DNABERT-2³⁰, HyenaDNA³¹) which handle multi-species sequences, and cross-modal variants (DNAGPT³², CD-GPT³³) that jointly learn from genomic, RNA and protein data. While LLMs have also shown success in predicting coding variant effects (e.g., AlphaMissense³⁴, ESM1b-based models³⁵), and other tools such as FABIAN-variant³⁶ focus on variant impact on TFBS using PWMs/TFFMs, there is a rising need for robust methods that specifically leverage LLMs to systematically integrate the genome-wide gene regulatory information and assess the impact of somatic short nucleotide variants across a comprehensive range of non-coding elements as they capture both distal and proximal regulatory contexts.

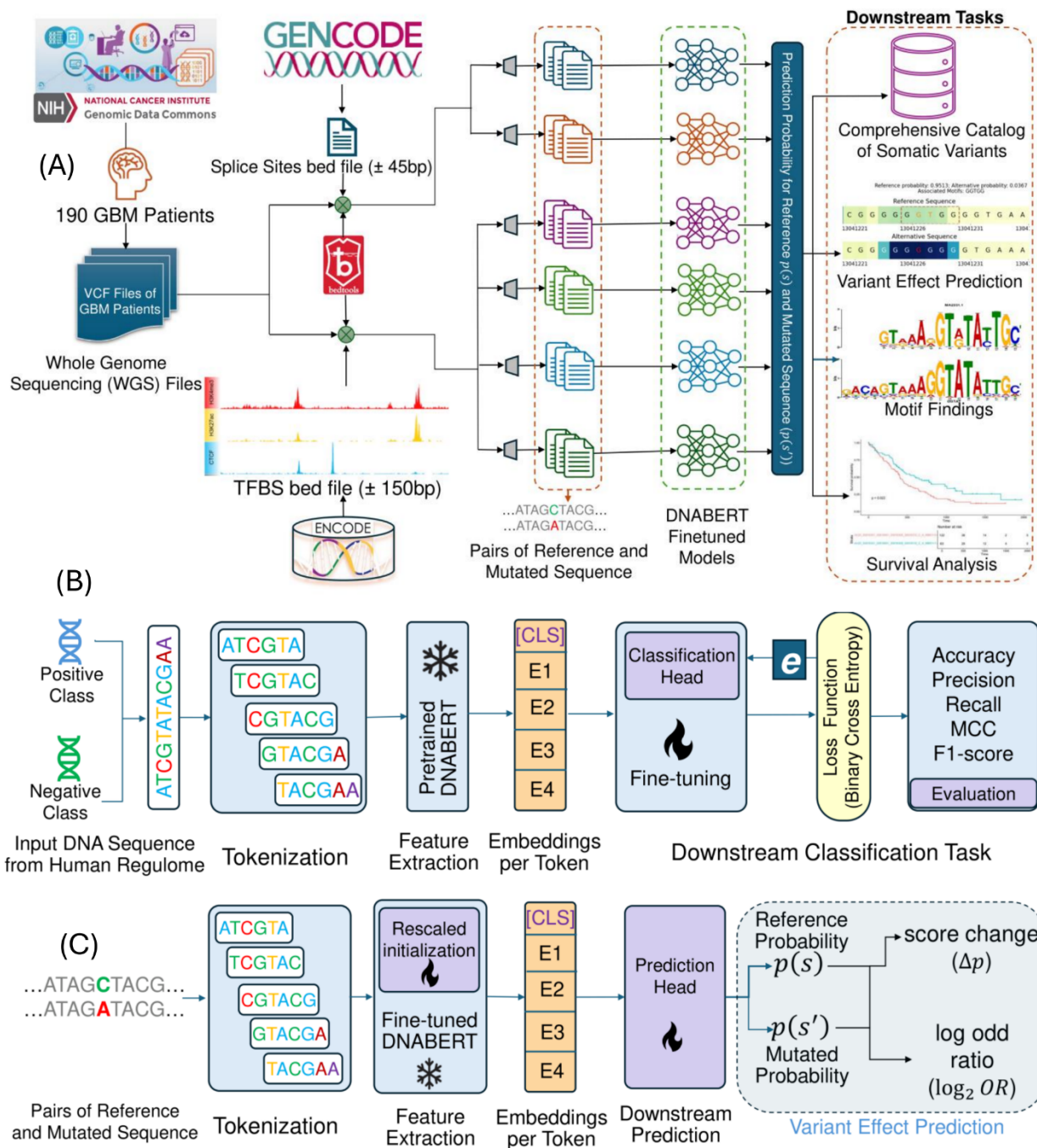


Figure 1: Architecture of **DeepVRegulome**. **(A)** Schematic of the computational framework: Starts with WGS and VCF data from 190 GBM patients (GDC). Splice site (GENCODE) and TFBS (ENCODE) annotations are intersected using BEDTools to define input regions, from which reference and mutated sequence pairs are extracted. High-impact variants are then cataloged for downstream analysis, including motif disruption and clinical annotation. **(B)** Pretrained DNABERT model is fine-tuned for regulatory prediction tasks using labeled data from donor/acceptor splice sites and ENCODE ChIP-seq peak regions. Fine-tuning is performed in two stages: transfer learning from the pretrained model (frozen or partially trainable) and training from scratch for each regulatory class. **(C)** Fine-tuned models are used to score somatic variants in GBM patient genomes by computing prediction probabilities on wild type ($p(S)$) and mutated sequences ($p(S')$). Variant disruption scores are derived via log-odds ratio and attention-based score change.

Despite recent advances, few studies implemented LLMs to systematically predict the effects of somatic mutations in non-coding regions, with existing tools often limited to small TFBS datasets and narrow genomic coverage. To address this methodological gap, we developed **DeepVRegulome**, a deep-learning framework integrating DNABERT-based²⁷ genomic foundation models, to systematically predict and characterize the functional impact of short genomic variants on both splice sites and a vast array of cis-regulatory elements, utilizing over 700 TFBS datasets from The Encyclopedia of DNA Elements (ENCODE) database³⁷. We selected DNABERT over more recent models

like DNABERT-2 and Segment-NT due to its comparable performance on short sequences (less than 300bp) relevant to these regulatory elements. Our framework fine-tunes DNABERT using two main sources of regulatory information: acceptor/donor splice sites from GENCODE and hundreds of CHIP-seq datasets from ENCODE for transcription factors and histone marks. This process yields highly accurate models designed to predict the functional impact of somatic mutations. DeepVRegulome further integrates quantitative variant scoring (log-odds ratios, score-change values), attention-based motif analysis for identifying disrupted motifs, and interfaces with established variant databases like dbSNP³⁸ and ClinVar³⁹ for clinical context.

We applied DeepVRegulome to WGS from 190 glioblastoma tumors⁴⁰⁻⁴⁴, an aggressive brain cancer with limited therapeutic options, to demonstrate its utility in a complex disease setting. Glioblastoma's poor prognosis and the known role of non-coding mutations in oncogenesis make it an ideal testbed for this approach^{41, 45, 46}. Our analyses identified thousands of high-impact variants recurring across patients, including those disrupting critical regulatory elements linked to patient survival outcomes. The resultant variant signature robustly stratifies glioblastoma patients, highlighting clinically relevant non-coding mutations that are potentially valuable for therapeutic targeting^{47, 48}. This study aims to provide a framework for uncovering novel, functionally significant non-coding mutations in all types of cancer, thereby offering new perspectives for precision oncology. In summary, **DeepVRegulome** represents a significant methodological advancement for interpreting non-coding somatic mutations, providing a powerful, generalizable tool for cancer genomics and precision oncology. Our openly accessible framework and interactive results dashboard facilitate future research into the regulatory genome, promoting broader adoption and extending utility to other cancer types and genomic studies.

Results

DeepVRegulome is an integrated computational framework composed of four distinct modules designed to systematically predict and interpret the functional impact of non-coding variants (Figure 1).

1. Regulatory Region Prediction Module:

To perform accurately *in silico* mutagenesis experiments on short DNA sequences, we need highly accurate classification models for predicting functional gene regulatory DNA sequences. We developed DNABERT-based fine-tuned models for predicting regulatory regions of two different sizes, (i) ± 45 bp region flanking splice sites and (ii) ± 150 bp region flanking CHIP-Seq (for TFBS and histone marks) or RNA Bind-n-Seq peak regions, covering 23% of the human genome.

The splice site models demonstrated high predictive accuracy across multiple metrics (Accuracy: 94–96%; F1-score: 0.94–0.96; MCC: 0.89–0.92; Figure 2f). This performance underscores DNABERT's capability to learn the complex sequence features surrounding canonical splice junctions. For ENCODE regulatory elements, we fine-tuned models on CHIP-seq peak regions for 667 TFs and 33 histone marks; we also designated 59 of the TFs as RNA-binding proteins (RBPs) based on their known functions⁴⁹. We included only those fine-tuned models that surpassed 85% accuracy. While 421 TFs (~63% of all evaluated) and 37 RBP models achieved this accuracy, only 4 histone marks (H4K12ac, H2AK9ac, H3K9me1, and H3K23me2) were included in the final set of fine-tuned models. This demonstrates the strong ability of DNABERT fine-tuned models to learn sequence-specific patterns in TF target regions. In contrast, performance was more variable for histone marks, suggesting that their positioning may be governed by factors beyond local sequence content that are not fully captured by the current models.

The top-performing TFBS model (CTCFL⁵⁰) achieved close to perfect accuracy (0.9838), followed by ZNF426⁵¹ (0.9709), SAFB⁵² (0.9702), RBM34⁵³ (0.97) and TAF15⁵⁴ (0.9674). These results confirm the robustness and specificity of DNABERT models across a wide diversity of TFs, including both canonical regulators (e.g., SPI1, E2F6, MITF, USF1) and RNA-binding proteins (SRSF3, RBM14, PCBP1). As shown in the boxplots (Figure-2a), TF models and RNA-binding proteins consistently demonstrated high predictive performance across all metrics, while histone marker models, although fewer in number, also achieved robust classification with slightly broader variance. Receiver operating characteristic (ROC) curves for the top 15 TFBS models (Figure-2c) revealed exceptional discriminative power (AUC > 0.97), further supported by radar plots (Figure-2b) indicating uniformly high recall and MCC values across top-performing models. Evaluation loss trajectories confirmed stable convergence and generalization across training epochs (Figure-2f). In parallel, all four histone marker models exhibited strong ROC performance (AUC range: 0.94–0.96; Figure-2e), demonstrating that the fine-tuned models in this module effectively capture regulatory signals at base-pair resolution for both transcription factors and chromatin features.

These results establish the robustness and discriminative capacity of DeepVRegulome for modeling TF-specific DNA binding signatures, even under the variability and noise inherent to CHIP-seq data. The consistent performance across both broadly expressed and tissue-specific TFs demonstrates the framework's suitability for downstream variant impact prediction. Collectively, the high-fidelity models for both splice sites and TFBSs form the predictive backbone of DeepVRegulome, enabling reliable assessment of non-coding variant effects in disease-relevant contexts.

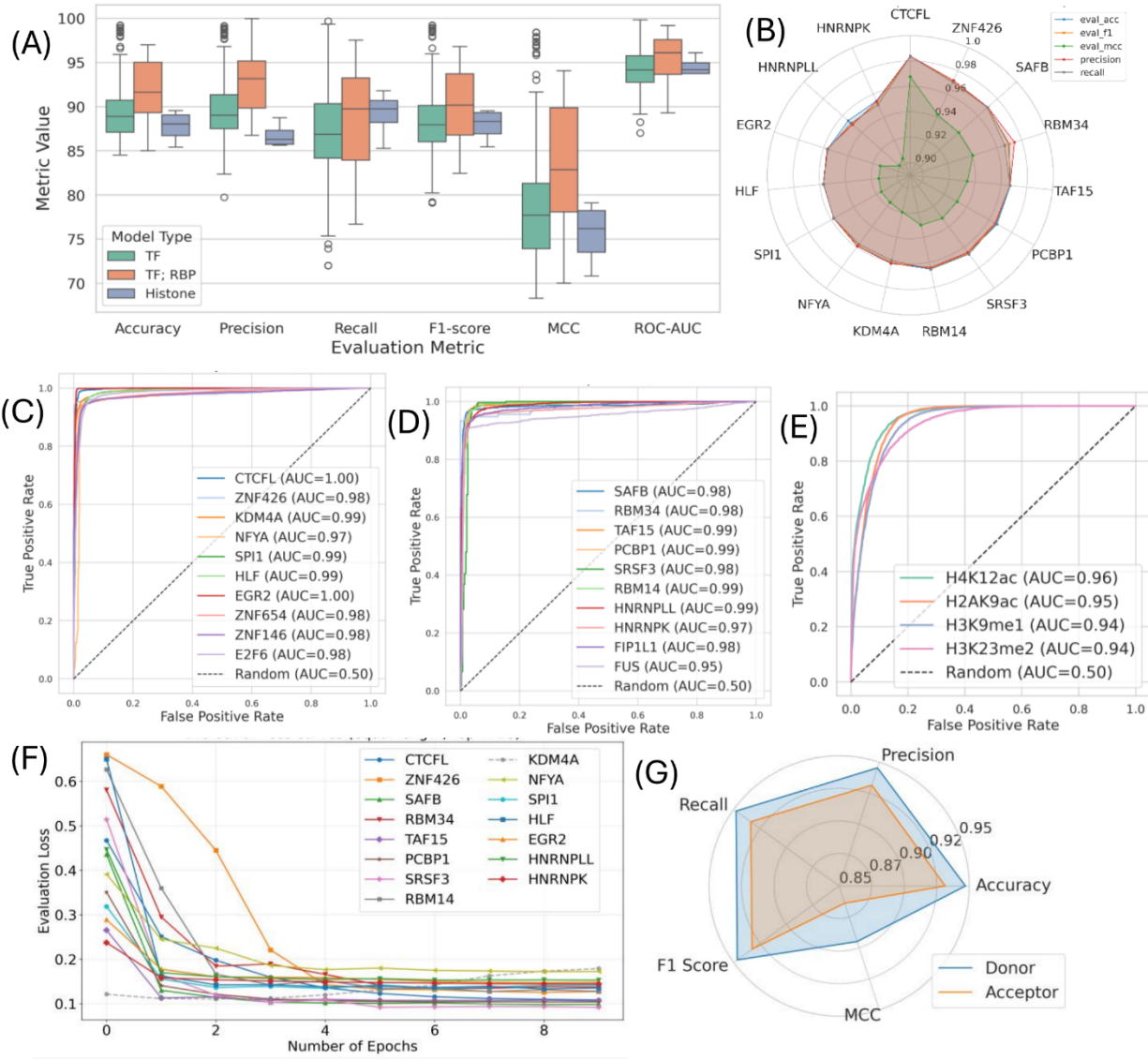


Figure 2: **Performance of DeepVRegulome models in predicting diverse regulatory elements.** (a) Boxplots comparing six evaluation metrics across fine-tuned models for transcription factors (TFs; $n = 421$), RNA-binding proteins (RBPs; $n=37$), and histone marks ($n = 4$). The results highlight consistently high performance for TF and RBP models and more variable performance for histone mark models. (b) Radar plot showing multi-metric performance of the top 15 TFBS models, selected based on evaluation accuracy, revealing uniformly high recall and MCC across top performers. (c,d) ROC curves for the top 15 TFBS models (c) and top 15 RBP models (d) demonstrate excellent discriminative ability, with AUC values ≥ 0.98 and ≥ 0.95 , respectively. (e) ROC curves for all four histone marker models which having evaluation accuracy greater than 85%, indicating slightly lower but still robust classification performance. (f) Evaluation loss trajectories across top 15 TFBS models, showing steady convergence and stable generalization behavior. (g) Comparative radar plot between donor and acceptor splice site classifiers across five evaluation metrics, emphasizing trade-offs between precision and recall. Collectively, these results highlight the robustness and generalizability of DeepVRegulome across diverse classes of regulatory elements.

2. In silico Mutagenesis Module:

The main objective of this module is to predict the effects of short variants on a regulatory sequence, such as TF or histone bound region, splice sites, or RBP binding sites. First, the mutation information from VCF files is integrated with ENCODE regulatory regions and splice sites to find all the mutated regulatory regions in the genome. For a given regulatory sequence with mutations, we systematically change the nucleotides within a sequence and use a computational model to predict the resulting change in the sequence's function or property based on predictive probability or score changes from the corresponding fine-tuned model compared to the reference sequence.

Table 1: Summary of total number of variants in the regulatory regions and predicted functional variants and affected regulatory regions across splice site and ChIP-seq-based fine-tuned DNABERT models.

Fine-tuned models	Subtype	Variant Type	Number of		Predicted variants and regulatory regions	
			Variants	Regions	Number of Variants (present in >10% of the samples)	Number of Regions (present in >10% of the samples)
Splice Sites	Acceptor	SNVs	19,968	14,743	299 (1)	265 (3)
		Indels	34,718	19,897	1,822 (437)	1,375 (408)
	Donor	SNVs	23,656	15,849	673 (4)	545 (4)
		Indels	20,171	13,491	504 (130)	423 (122)
ChIP-seq Models	Histone Markers	SNVs	127,297	57,013	387 (2)	311 (5)
		Indels	254,566	87,949	536 (150)	373 (129)
	TFs	SNVs	932,133	358,414	19709 (1087)	16566 (322)
		Indels	2,130,274	533,433	35867 (8598)	30411 (7,297)

We applied our fine-tuned models to predict the functional impact of short variants from 190 glioblastoma patients in the TCGA and CPTAC-3 cohorts. We analyzed variants within defined splice site regions (± 45 bp around junctions) and cis-regulatory regions (± 150 bp around ChIP-seq peak summits for TFBSs and histone marks). Then the functional impact was quantified using a log-odds ratio and a prediction score change between reference and mutated sequences. The analysis revealed a high burden of somatic mutations within non-coding regulatory elements, particularly in TFBS regions. Within these sites, we identified 932,133 SNVs mapped across 358,414 distinct regions and over 2.13 million indels mapped across 533,433 regions. DeepVRegulome predicted 35,867 indels and 19,709 SNVs to be functionally impactful in these regions, of which 8,598 indels and 1,087 SNVs were recurrent in $\geq 10\%$ of patients. The same analysis was performed for splice sites (acceptor and donor), histone markers, and transcription factor binding sites. A detailed summary of all identified variants, with further categorization for those predicted as functional and those recurring in more than 10% of patients, is provided in Table 1 and Supplementary Section S4.

Finally, we exclusively focus our biological and clinical analyses on predicted functional variants observed in $\geq 10\%$ of glioblastoma patients—a threshold chosen to balance the discovery of novel recurrent variants with sufficient statistical power for downstream analyses. To evaluate the relevance of these variants, we assessed their overlap with known entries in the dbSNP database and determined their location within known genes or splice site regions (Figure 5a, Supplementary Figure S3, Supplementary File S4).

3. Motif Visualization and Interpretation Module:

To facilitate model interpretability, DeepVRegulome includes a module for the post-hoc analysis of fine-tuned models. This module first derives candidate motifs from learned models, which are then subject to rigorous biological validation. Candidate motifs are identified via two primary strategies: statistical enrichment and attention-based analysis. First, we perform k-mer enrichment analysis between positively and negatively labeled sequences using a hypergeometric test, identifying cis-regulatory elements significantly overrepresented in ChIP-seq bound regions. In parallel, attention weight heatmaps from the DNABERT layers pinpoint salient nucleotides, from which sequence motifs crucial for model prediction can be extracted. This dual approach enables interpretability at both the sequence and variant levels, enhancing the biological relevance and explainability of DeepVRegulome predictions.

To assess the biological accuracy of the framework, we rigorously evaluated the motifs learned by our 462 high-confidence TF and RBP models against the JASPAR 2024 database. The comparison revealed that 402 of our 462 models (87%) learned motifs with significant similarity to a known JASPAR profile (Tomtom, $q \leq 0.05$). Remarkably, these validated models collectively recapitulated **~97%** (2256 of 2346) of the curated matrices in JASPAR, demonstrating comprehensive coverage of the known regulatory sequence space (Figure-3A).

For the 190 transcription factors present in both our ENCODE-derived catalogue and JASPAR 2024, a fine-grained analysis revealed high motif fidelity. Within this shared set, 132 (~72%) of the models learned motifs identical to their designated JASPAR counterparts (Supplementary Figure-S3). An additional 19 models (~10%) matched the known motif of a closely related paralogue from the same TF family. This is exemplified by the model for SP1, which learned a motif that strongly matched the JASPAR profile for its paralogue, Klf6-7-like ($q=2.89e-07$) (Figure-3C). This result correctly captures the conserved binding preference of the large Sp/KLF family, whose members share a canonical three-zinc-finger domain that recognizes GC-rich promoter elements. In total, 82% of this direct validation cohort (155 of 190) identified a biologically plausible binding preference. The remaining 35 models (~18%) represent potential discoveries of novel or alternative binding specificities for established TFs. Next, we characterized the remaining 272 models that lack a direct name match in the JASPAR database. The vast majority of these, 247 models (91%), still produced motifs with significant similarity to a JASPAR motif annotated to another TF, leaving 25 completely unmatched PWMs. A hierarchical breakdown of the validation results for all 462 models is provided in Figure- 3B.

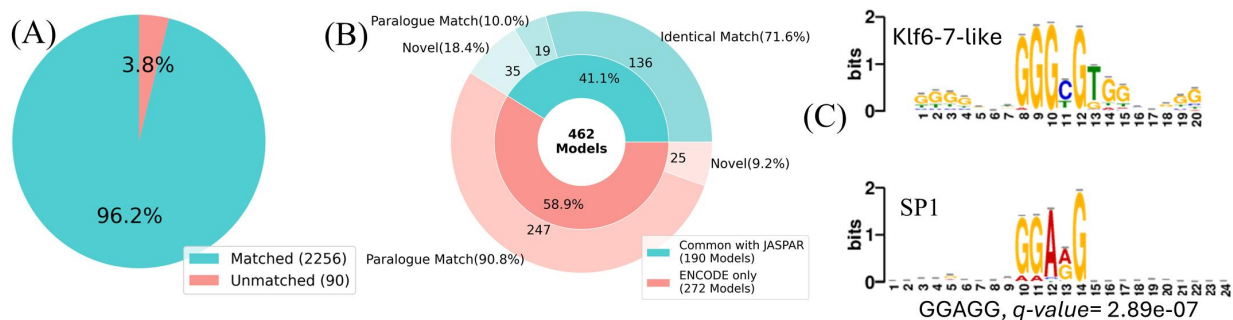


Figure 3: Large-scale validation and characterization of learned regulatory motifs. by DeepVRegulome. (A) Comprehensive coverage of the known regulatory sequence space. The 402 models with significant JASPAR similarity collectively recapitulate 96.2% (2,256 of 2,346) of the curated matrices in the JASPAR database. (B) Hierarchical breakdown of 462 high-confidence models following comparison to the JASPAR 2024 database (Tomtom, $q \leq 0.05$). The inner ring shows the initial split between models for TFs common to both ENCODE and JASPAR ($n=190$) and those unique to the ENCODE-derived set ($n=272$). The outer ring details the validation results for each group, classifying motifs as identical matches, paralogue matches, or novel. Percentages indicate the proportion within each of the two primary groups. (C) Example of a high-confidence paralogue match. The motif learned by the DeepVRegulome model for SP1 is shown below the JASPAR motif for its paralogue, Klf6-7-like. The strong visual similarity and statistical significance ($q=2.89e-07$) demonstrate the framework's ability to correctly identify the conserved DNA-binding preference of the Sp/KLF transcription factor family.

Adding these to the confirmed set means 402 of our 462 TFs ($\approx 87\%$) display clear motif similarity to some JASPAR matrix. The final 60 TF models (13% of the total), 35 common TF and 25 from TFs not annotated in JASPAR, show no convincing match and therefore represent the most promising candidates for novel or poorly characterized binding patterns.

However, the model's capability extends beyond simple motif matching to provide deeper biological insights into how these sequences function. For example, a G>C variant within an ETS1 motif upstream of the *GATAD2B* gene was shown to disrupt the core CCCGA sequence, which directly corresponded to an attenuation of DNABERT's attention scores at that site (Fig. 4B). These results confirm that *DeepVRegulome* does not merely achieve high performance in classification but also captures biologically interpretable features aligned with established regulatory signatures. This interpretability module thus bridges deep learning predictions with biological knowledge, allowing researchers to assess not only whether a variant is impactful, but also why—by tracing predictions back to recognizable motif regulatory grammar.

4. Survival Analysis and Patient Stratification Module:

To assess the clinical relevance of the variants identified by DeepVRegulome, we performed survival analysis and found that predicted functional disruptions in both TFBSs and splice sites were significantly associated with patient outcomes. For TF binding sites, we found that the vast majority of these clinically relevant variants represent novel findings. An evaluation against the ClinVar database revealed that only 13 significant indel variants from our top TFBS models had a prior clinical entry, with no SNVs having a record. The few variants that were found occurred in TFs with established roles in cancer progression. These included key regulators such as SMAD4 (role in pathways like TGF- β signaling)⁵⁵ and FOXM1, which drives cell proliferation, particularly in oncogenesis. The discovery of these functionally impactful variants, despite their absence from clinical databases, highlights a central point: there is a large, clinically uncharacterized landscape of non-coding mutations that DeepVRegulome can help prioritize.

Disruptions in TFBSs also showed strong correlations with clinical outcomes. For example, a substitution in a PNOX1 TFBS within the gene *TLK2* was associated with significantly worse survival ($HR = 2.3$, $p = 2.7 \times 10^{-3}$). *TLK2* has recently been cited as a potential therapeutic target, inhibitors of which have efficacy in several cancer cell lines⁵⁶. Similarly, a deletion in a RELB TFBS within the *ZDHHC8* gene, which is correlated with worse survival when highly expressed, also predicted poorer outcomes ($HR = 2.1$, $p = 1.2 \times 10^{-4}$)⁵⁷. Conversely, an insertion in a SP1 TFBS upstream of a transcript of the gene *PRKCE* was associated with better survival ($HR = 0.46$, $p = 2.5 \times 10^{-2}$). Protein Kinase C and its isozymes have been intensely studied as therapeutic targets in Glioblastoma⁵⁸⁻⁶⁰. However, very few works in the literature study *PRKCE* and its transcripts, suggesting the need for further research. Our analysis also revealed mutations near the genes *SPBTN4* ($HR = 1.7$, $p = 3.6 \times 10^{-3}$) and *C3orf20* ($HR = 0.65$, $p = 1.5 \times 10^{-2}$) that are associated with survival and with changes in expression. Though both genes are indicated in other cancers, their connection with GBM has not been studied (Figure 4D, E). In addition, TFBS disruptions in immune-related genes *TRBV5-4* ($HR = 2.0$, $p = 6.5 \times 10^{-3}$) and *TFAP2A* ($HR = 2.3$, $p = 2.8 \times 10^{-4}$) are also negatively associated with survival.

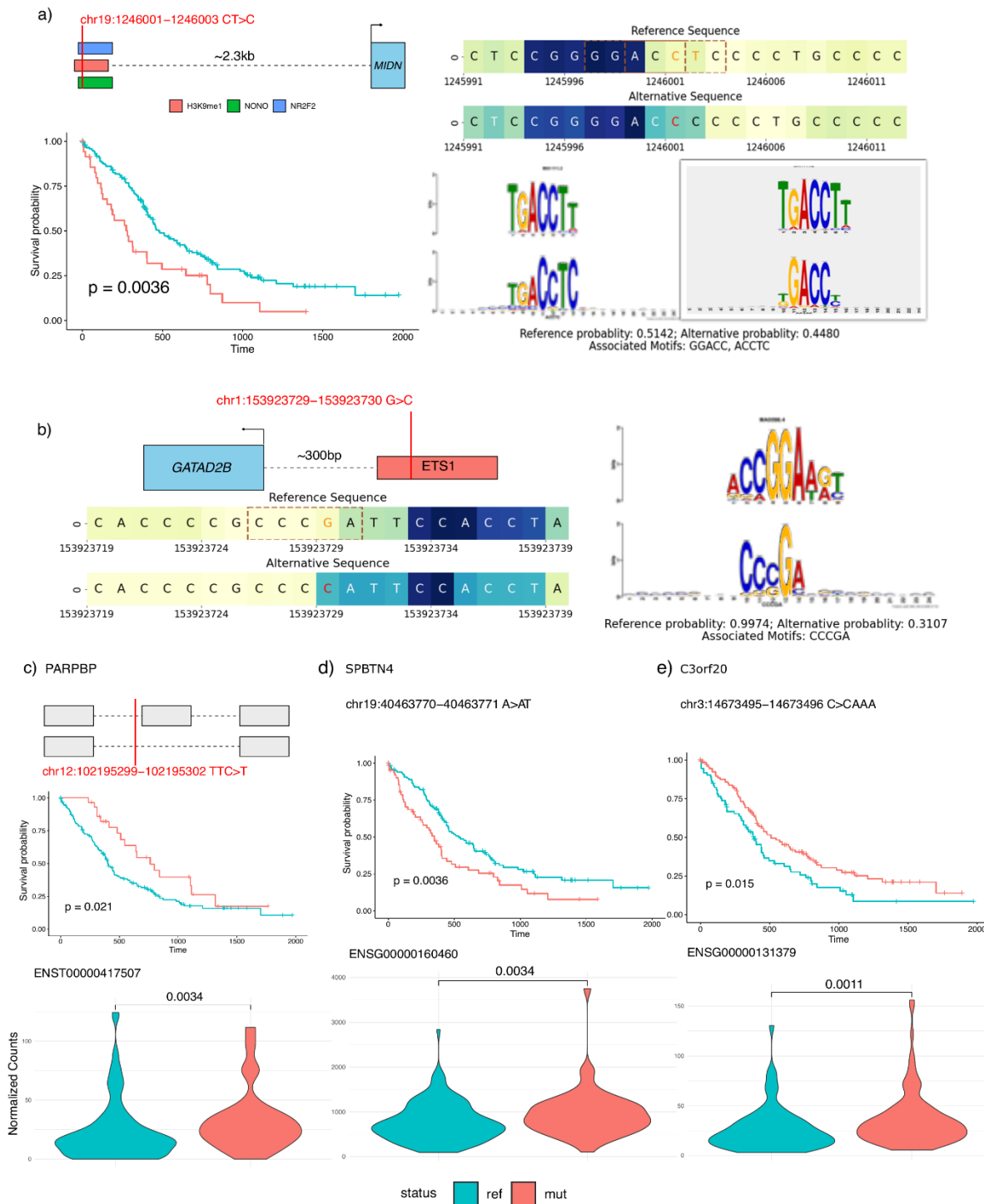


Figure 4: Integrative analysis of high-impact non-coding variants and their association with clinical outcomes in glioblastoma. (A) A CT>C substitution in a predicted NR2F2 binding site located ~2.3kb upstream of the MIDN gene. The mutation is predicted to be disruptive, as shown by the attention score heatmaps (right). Kaplan-Meier analysis (left) shows that patients harboring this variant have significantly worse overall survival ($p = 0.0036$). (B) A G>C substitution in a predicted ETS1 binding site located ~300bp upstream of the GATAD2B gene. The model predicts a strong disruption of the core motif, with binding probability dropping from 0.99 to 0.31. (C) A TTC>T variant in a splice site region is associated with worse patient survival ($p = 0.021$) and is linked to significantly increased expression of a transcript missing an exon downstream of the disruption, ENST00000417507 ($p = 0.0034$). (D) An A>AT insertion is associated with worse survival ($p = 0.0036$) and a significant increase in the expression of the gene SPBTN4 ($p = 0.0068$). (E) A C>CAAA insertion is associated with worse survival ($p = 0.015$) and a significant increase in the expression of the gene C3orf20 ($p = 0.0021$).

To showcase the framework's integrative power, we highlight a G>C somatic variant within a predicted NR2F2 motif (chr1:153923729; Figure. 4A). The mutation disrupts the canonical GGACC/ACCTC pattern (JASPAR, $p = 1 \times 10^{-3}$), reduces model attention at the site, and lowers the predicted NR2F2 binding probability. This predicted functional disruption correlated strongly with clinical outcomes; Kaplan–Meier analysis shows that carriers of the mutant allele have significantly shorter survival (log-rank $p = 0.0036$). This TFBS lies less than 5 kb upstream of *MIDN*, a neurodevelopmental gene⁶¹, suggesting a potential GBM-relevant regulatory mechanism⁶²(Figure 4A).

We also analyzed variants in splice sites for their association with survival. Within splice sites, a mutation in the acceptor site of PARPBP⁶³ (PARP1 binding protein) was linked to improved survival (HR = 0.54, $p = 0.02$). This finding is supported by isoform expression analysis, which showed an increase in an isoform that excludes the downstream exon (Figure 4C), consistent with the predicted acceptor site disruption⁶⁴. In contrast, a mutation in the donor site of MAPT (Tau) was associated with worse survival (HR = 1.7, $p = 0.0077$)^{65, 66}. This also aligned with isoform expression data, where an increase in an isoform that skips the first exon was observed in mutants, as predicted by our model. A comprehensive list of all survival-associated variants and regions is available in Supplementary notes S2 and S3.

DeepVRegulome Identifies Biologically Relevant TFBS Variants in GBM: Our analysis highlights several candidate variants predicted by DeepVRegulome in both TFBS and splice site regions, which possess substantial biological relevance, particularly in pathways critical to disease pathogenesis and progression. We assessed these candidate variants in TFBS regions using two complementary approaches: first, by identifying TFBS models with the highest evaluation accuracy; and second, by focusing on TFBS models predicting the highest number of candidate variants. In both strategies, we prioritized models exhibiting both substantial variant counts and established roles in gene regulation and cancer biology.

For the first approach, the top 35 TFBS models based on evaluation accuracy are shown in a sunburst plot for SNVs (Figure-5B) and indels (Figure-5C), where right hand horizontal x-axis showing the highest accuracy of TFBS model, and it decrease anticlockwise. Analysis of these top-performing TFBS models revealed hundreds of candidate variants affecting TFs with established roles in neurodevelopment, immune regulation, and cancer. Notable examples include *EGR2*³⁹, a critical factor in nerve cell differentiation; *SPI1*⁶⁷, which is crucial for immune system function; *ZIC2*⁶⁸, a factor implicated in glioblastoma tumor progression; and *CTCF*⁶⁹, which is involved in cancer-associated chromatin remodeling.

In the second approach, we summarize the candidate variants and their associations from the top TFBS models based on the number of predicted candidate variants. Among the 460 TFBS models, the top 50 models for predicting candidate variants are presented as stacked bar plots in Figure 5. The y-axis of the stacked bar plot represents the combined count of significant indel variants (Figure 5(E)) and SNV variants (Figure 5(D)), along with their associated DBSNP counts. The secondary y-axis, located on the right-hand side, depicts model accuracy as a line plot. For SNV variants, the top 5 TFBS models based on candidate variant counts are NONO⁷⁰ (87.40%), RAD51^{50, 71, 72} (87.06%), ZBTB33⁷³ (86.78%), IKZF2 (86.79%), SMARCE1⁷⁴ (86.71%), which identify 93, 78, 69, 50, and 48 significant SNV variants, respectively. These SNVs are associated with 87, 76, 67, 49, and 44 DBSNP entities. In terms of indel variants, the top 5 TFBS models based on candidate variant counts are ZNF384⁷⁵ (88.58%), FOXA1 (88.52%), ZBTB33 (86.78%), MTA2⁷⁶ (85.15%), and NR3C1 (85.91%), which identify 368, 201, 148, 134, and 132 significant indel variants, respectively. These indels are associated with 158, 120, 115, 57, and 99 DBSNP entries. ZBTB33 (also known as Kaiso)⁷³—the top-ranked model by both SNV and indel counts—is a CpG-methylation-dependent repressor that links epigenetic marks to transcriptional control, notably regulating Wnt-signalling genes implicated in cancer.

Further, our analysis pinpointed transcription factors with significant, known roles in glioblastoma biology. *STAT3*⁷⁷, a key oncogene in glioblastoma, was found to have 66 significant indel variants in its binding sites. Disruptions were also numerous in the binding sites of *FOXA1*⁷⁸ and *CREB1*⁷⁹, which are involved in tumor invasion and proliferation. *RFX1*⁸⁰, another immune-related factor, is essential for MHC class II gene regulation, with implications in immune-mediated cancers and potential relevance to glioblastoma through its regulatory influence on immune pathways. Together, these TFBS models represent critical factors in cancer progression, chromatin remodeling, and immune response modulation, providing insights into pathways essential for glioblastoma and other cancer studies. A comprehensive analysis of the top 462 TFBS models for each approach is provided in Supplementary **Table-S1**.

Discussion

DeepVRegulome provides a unified deep-learning framework for genome-wide analyses of short variants for prioritization and interpretation of functionally disruptive candidate variants in the non-coding regulatory genomic

regions. DNABERT fine-tuned models, trained on the human regulome consisting of target regions of 700 different TFs, histone proteins and RBPs and splice-junction regions, integrates gene-regulatory information with high predictive

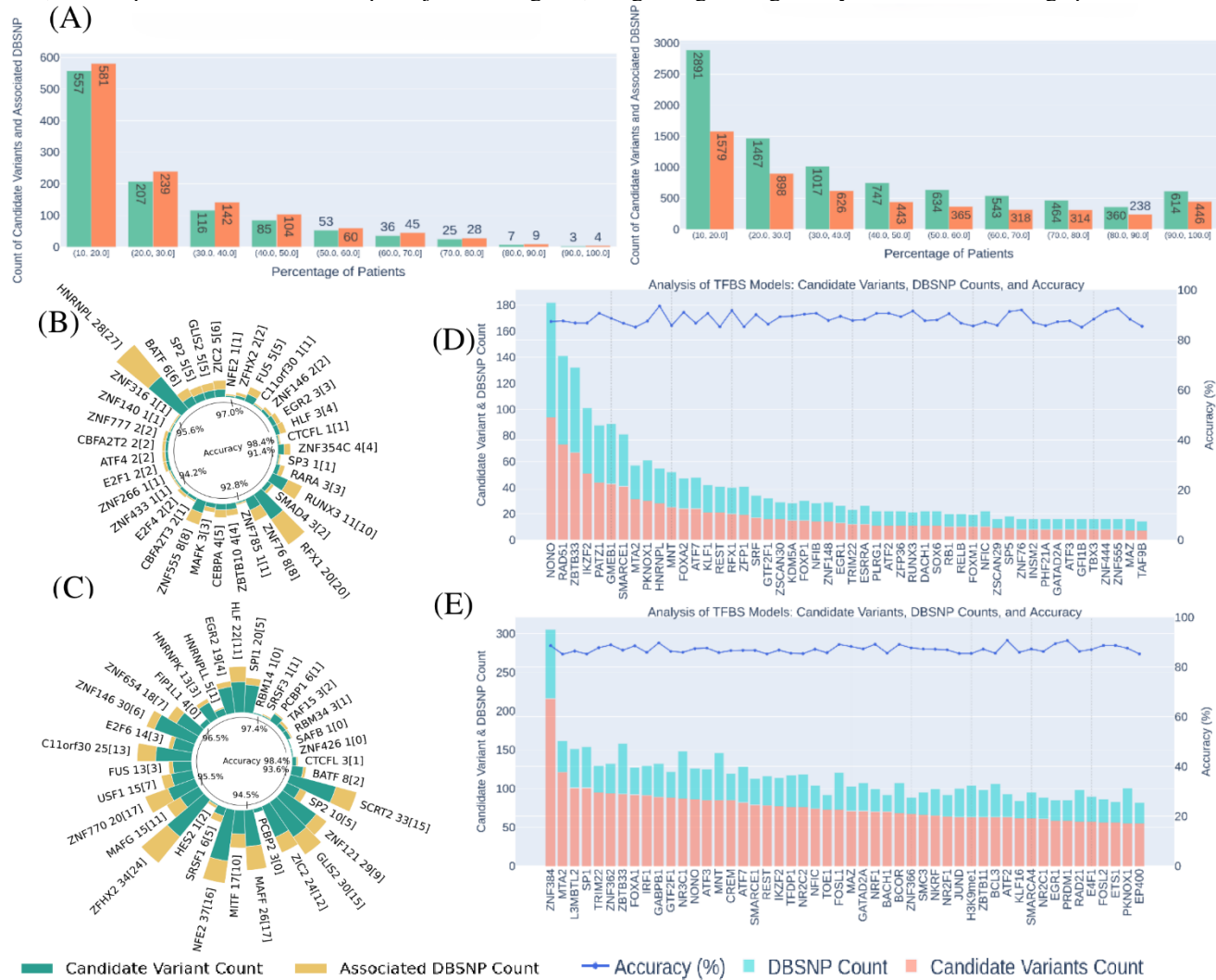


Fig 5: (A) Distribution of candidate and dbSNP-associated variants across GBM patients, stratified by the percentage of individuals affected. Left: CaVEMan SNVs; Right: Sanger Pindel indels. Candidate variants (green) and dbSNP variants (orange) are plotted per patient frequency bin, revealing that SNVs are more often annotated in dbSNP, while indels are predominantly novel. (B, C) Circular representation of the top 50 TFBS models based on model performance, sorted in decreasing order of evaluation accuracy. Each bar represents a TFBS model and is labeled as: *TFBS_model_name Candidate_Variant_Count [DBSNP_Count]*. Green bars indicate the number of candidate variants, yellow bars show associated dbSNP counts. Panel (B) shows CaVEMan SNVs, and panel (C) shows Sanger Pindel indels. (D, E) Comparison of the top 50 TFBS models based on the distribution of candidate variants, dbSNP counts, and model accuracy. Stacked bar plots show the number of candidate and dbSNP variants for each TFBS model (sorted in decreasing order of candidate variant count), while a blue line indicates model accuracy on a secondary y-axis. Panel (D) represents CaVEMan-based SNVs, and panel (E) represents Pindel-based indels.

accuracy across diverse regulatory contexts (Figure-2). Unlike classical motif-scanners that rely on fixed position-weight matrices and early deep-learning models that were trained for a single regulatory class, DeepVRegulome deploys element-specific transformer models for splice sites, TFBSs and histone marks in a single framework, capturing longer-range sequence grammar than previous methods^{23, 81, 82}. Importantly, we showed that the framework is not a "black box"; its integrated interpretation module learns biologically meaningful features, such as the successful rediscovery of known TF motifs from the JASPAR database. Applied to 190 glioblastoma cancer genomes, the approach prioritized ~59,000 high-impact variants, of which >10,000 recur in $\geq 10\%$ of patients and are associated with overall survival (Supplementary Table S4). These results demonstrate that modern genome foundation models can bridge the gap between variant discovery and biological interpretation in large, clinically heterogeneous complex disease cohorts.

The strengths of DeepVRegulome can be categorized into three key areas. First, its region-specific fine-tuning strategy yields superior performance on short regulatory windows, enabling precise localization of motif disruptions. Second, the attention-guided interpretability module recovers canonical motifs de novo (Fig. 3) and links variant-level attention loss to experimentally validated TF motifs, providing mechanistic insight beyond probabilistic scores. Third, the pipeline integrates variant recurrence, dbSNP overlap and Kaplan–Meier statistics, converting sequence-level disruptions into clinically actionable signatures. For example, a G→C mutation that abolishes an *NR2F2* motif upstream of *MIDN* stratifies patient survival (log-rank $p = 0.0036$; Figure-4A), while an acceptor-site SNV in *PARPBP* predicts improved outcome and suggests heightened sensitivity to *PARP* inhibition. Such findings highlight how the framework can guide novel therapeutic hypothesis-driven targets directly from WGS data.

A major finding of this study is the large "annotation gap" for functional non-coding variants. We found that the vast majority of the high-impact, recurrent variants identified by DeepVRegulome are not recorded in clinical databases like ClinVar. The few that were found, such as in the TFBSs for *SMAD4* and *FOXMI*, occurred in TFs with well-established roles in cancer progression. This highlights a vast, clinically uncharacterized landscape of potentially pathogenic non-coding variants and establishes DeepVRegulome as a powerful discovery tool for prioritizing these variants for future clinical annotation and research. Beyond oncology, DeepVRegulome is readily extensible to germline rare-disease sequencing, population-scale variant catalogues and multi-modal datasets that include methylation or chromatin-accessibility profiles. The open-source code, trained weights and interactive dashboard (Data availability) lower the barrier for community adoption and for benchmarking against emerging foundation models. We anticipate that systematic application of DeepVRegulome across large consortia cohorts—such as PCAWG, TCGA-PanCancer and UK Biobank—will yield a comprehensive atlas of functional non-coding mutations, thereby accelerating variant prioritization for precision medicine.

Several limitations necessitate further discussion. Our current implementation uses 300-bp windows, which may miss distal enhancer–promoter interactions and long-range chromatin loops. This local focus is also the likely reason for the framework's lower performance on most histone marks compared to TFBSs; histone modifications are often governed by broader regional context or DNA shape rather than the specific local motifs our model excels at identifying. Extending to context-aware models such as DNABERT-2 or HyenaDNA^{7,8}—and incorporating Hi-C-derived contact priors—should improve detection of distal regulatory effects. Our study is confined to glioblastoma; although the model architecture is agnostic to tumor type, additional cancer cohorts will be required to assess generalizability and to refine recurrence thresholds. Finally, our functional validation is confined to in-silico motif disruption, RNA-seq isoform shifts, and survival correlations; establishing causality will require orthogonal wet-lab assays—such as allelic luciferase or minigene reporters, CRISPR base-editing of glioblastoma lines, and single-cell transcriptomics—to confirm that the identified variants directly perturb regulatory activity.

In summary, DeepVRegulome couples high-fidelity regulatory modelling with transparent interpretation and clinical association, establishing an end-to-end path from raw whole-genome sequencing to biologically and clinically meaningful variant sets. By illuminating the regulatory genome at single-nucleotide resolution, the framework advances our ability to decipher the non-coding mutational landscape and highlights new avenues for translational genomics.

Methods

DeepVRegulome Architecture overview

We fine-tuned DNABERT on two task-specific corpora—90-nucleotide sequences centered on GENCODE v41 exon–intron junctions for splice-site recognition and 301-nucleotide sequences centered on ENCODE peak summits for 700 TFBSs. For splice sites we trained separate acceptor and donor models, while for TFBSs we trained one model per transcription factor, yielding 700 task-adapted classifiers. In each task, the curated sequences constitute the positive class, whereas length-matched sequences random sampled from the remainder of the mappable genome form the negative class. A detailed description of the fine-tuning data collection is provided in the "Data Acquisition" section. Detailed parameters and procedures for the DNABERT fine-tuning process, including k-mer tokenization, encoder architecture, classification head design, training regimen, hyperparameter optimization, and performance evaluation metrics, are provided in **Supplementary file S1**.

Variant Impact Prediction and Scoring

Once we finalized the selection of the best finetuned models, every substitutions or indel located within the corresponding non-coding regions was evaluated. To achieve this, a systematic data preprocessing workflow was established to prepare the datasets for input into these finetuned DNABERT models. The process began by identifying variants located within splice sites and TFBS regions using the bedtools⁸³ intersect module, effectively pinpointing mutations within these critical non-coding regions. For every intersecting event we constructed a matched sequence pair: the reference (wild type) sequence (s) and the corresponding mutated sequence (s'), bearing the alternative allele. These sequence pairs constituted the inputs for the fine-tuned DNABERT models in all downstream scoring analyses.

A variant was classified as functionally disruptive if the model's posterior probability ($p(s)$) of the wild type was greater than 0.5 and the probability of the mutated sequence ($p(s')$) was less than 0.5. Disruption magnitude is quantified using two complementary statistics: score change²⁴: $S = \Delta p = (p(s') - p(s))\max(p(s'), p(s))$, where the max term is added to amplify the strong effects of genetic variants; and log odds ratio²⁵ $\log_2 OR = \log_2 \frac{p(s)}{1-p(s)} - \log_2 \frac{p(s')}{1-p(s')}$, which reflects the association between events “being classified as a positive” and “having the particular genetic variant”(Figure-1C). A larger log odds ratio (>0) indicates that the variant results in a more impactful functional disruption.

Output and Application

This pipeline converts raw WGS data into quantitative estimates of regulatory disruption. The resulting catalogue comprises per-variant probability shifts, Δp scores and log₂-odds ratios for every splice-site and TFBS mutation observed across our glioblastoma cohort, enabling direct prioritization of non-coding variants for downstream survival analysis, motif interrogation and experimental validation. Applying DeepVRegulome thus uncovered candidate variants with putative effects on gene regulation and splicing in glioblastoma, offering new insights into the contribution of non-coding variation to tumor biology.

Datasets

To investigate the functional impacts of somatic genetic variants in non-coding regions associated with glioblastoma multiforme (GBM), we assembled three primary datasets:

- a) *Whole-Genome Sequencing (WGS) Data for glioblastoma Patients*
- b) *Splice Site Sequences*
- c) *Transcription Factor Binding Site (TFBS) Data*

Whole-Genome Sequencing Data for glioblastoma Patients: We retrieved WGS data for glioblastoma patients from the Genomic Data Commons (GDC) Data Portal⁸⁴. Specifically, sequencing data for 190 patients were obtained from the CPTAC-3 and TCGA-glioblastoma cohorts (**Supplementary Figure S2a**), which are extensively characterized and widely utilized in cancer genomics research. For each patient, we acquired two types of variant call format (VCF) files⁸⁵: one generated using the CaVEMan variant caller⁸⁶ and another using Pindel⁸⁷.

Splice Site and Transcription Factor Binding Site Data: For the splice site analysis, exon-intron junction sequences were sourced from the GENCODE project (version 40)⁸⁸. Each junction was extended by 45 nucleotides upstream and downstream to generate sequences of consistent length (90 bp) suitable for DNABERT input, resulting in hundreds of thousands of acceptor and donor windows. For the transcription factor binding site (TFBS) analysis, binding site data were obtained from The Encyclopedia of DNA Elements (ENCODE) database³⁷, comprising 4,228 ChIP-seq experiments for 667 TFs and 33 histone marks. Sequences were standardized to 301 bp, including 150 base pairs upstream and downstream of the binding site, to ensure consistent input length for model training. Further details on dataset processing, characteristics, and summary statistics are provided in Section S2 of supplementary material and Supplementary Figure S1 and S2.

Code and data availability

The DeepVRegulome source code is available at <https://github.com/DavuluriLab/DeepVRegulome>. Fine-tuned model checkpoints and intermediate files will be deposited in Zenodo and released under a CC-BY-NC licence upon article acceptance; they are available from the corresponding author upon reasonable request during peer review. An interactive web application for exploring candidate variants, associated survival data, and gene-level information is accessible at <https://deepvregulome.streamlit.app>.

Conclusion

In this study, we present *DeepVRegulome*, a scalable and interpretable deep learning framework for prioritizing functional somatic mutations in non-coding regulatory regions of the human genome. By fine-tuning DNABERT, a genomic foundation model, on splice sites and over 700 TFBS datasets from ENCODE, we demonstrate high-fidelity predictions across multiple regulatory elements. DeepVRegulome's visualization and interpretation module offers biological insights by uncovering sequence motifs and attention patterns aligned with known transcription factor binding sites. Applying our method to glioblastoma WGS data, we uncover a catalog of recurrently mutated regulatory regions, many of which show clinical relevance through survival stratification. Importantly, the design of DeepVRegulome is modular and data-agnostic, making it readily applicable to a broad range of cancer types and other complex diseases beyond GBM. Its architecture enables seamless extension to new regulatory elements, variant types, and even multi-omics contexts. Collectively, DeepVRegulome bridges the gap between large-scale genome sequencing and functional interpretation of the non-coding genome, establishing a path toward precision oncology and pan-disease variant prioritization rooted in regulatory architecture.

References

1. Ng, P.C. & Kirkness, E.F. Whole genome sequencing. *Methods Mol Biol* **628**, 215-226 (2010).
2. Hubschmann, D. & Schlesner, M. Evaluation of Whole Genome Sequencing Data. *Methods Mol Biol* **1956**, 321-336 (2019).
3. Roepman, P. et al. Clinical Validation of Whole Genome Sequencing for Cancer Diagnostics. *J Mol Diagn* **23**, 816-833 (2021).
4. Zhao, E.Y., Jones, M. & Jones, S.J.M. Whole-Genome Sequencing in Cancer. *Cold Spring Harb Perspect Med* **9** (2019).
5. The Lancet, O. Incorporating whole-genome sequencing into cancer care. *Lancet Oncol* **25**, 945 (2024).
6. Paul, D.S., Soranzo, N. & Beck, S. Functional interpretation of non-coding sequence variation: concepts and challenges. *Bioessays* **36**, 191-199 (2014).
7. Dietlein, F. et al. Genome-wide analysis of somatic noncoding mutation patterns in cancer. *Science* **376**, eabg5601 (2022).
8. Castro-Mondragon, J.A. et al. Cis-regulatory mutations associate with transcriptional and post-transcriptional deregulation of gene regulatory programs in cancers. *Nucleic Acids Res* **50**, 12131-12148 (2022).
9. Zhang, F. & Lupski, J.R. Non-coding genetic variants in human disease. *Hum Mol Genet* **24**, R102-110 (2015).
10. Bao, N., Wang, Z., Fu, J., Dong, H. & Jin, Y. RNA structure in alternative splicing regulation: from mechanism to therapy. *Acta Biochim Biophys Sin (Shanghai)* (2024).
11. Kalnina, Z., Zayakin, P., Silina, K. & Line, A. Alterations of pre-mRNA splicing in cancer. *Genes Chromosomes Cancer* **42**, 342-357 (2005).
12. Kim, H.K., Pham, M.H.C., Ko, K.S., Rhee, B.D. & Han, J. Alternative splicing isoforms in health and disease. *Pflugers Arch* **470**, 995-1016 (2018).
13. Liu, Q., Fang, L. & Wu, C. Alternative Splicing and Isoforms: From Mechanisms to Diseases. *Genes (Basel)* **13** (2022).
14. Tabarini, N. et al. Exploration of Tools for the Interpretation of Human Non-Coding Variants. *Int J Mol Sci* **23** (2022).
15. Wang, Z. et al. Performance Comparison of Computational Methods for the Prediction of the Function and Pathogenicity of Non-coding Variants. *Genomics Proteomics Bioinformatics* **21**, 649-661 (2023).
16. Avsec, Z. et al. Effective gene expression prediction from sequence by integrating long-range interactions. *Nat Methods* **18**, 1196-1203 (2021).
17. Askr, H. et al. Deep learning in drug discovery: an integrative review and future challenges. *Artif Intell Rev* **56**, 5975-6037 (2023).
18. Giri, S.J., Dutta, P., Halani, P. & Saha, S. MultiPredGO: Deep Multi-Modal Protein Function Prediction by Amalgamating Protein Structure, Sequence, and Interaction Information. *IEEE J Biomed Health Inform* **25**, 1832-1838 (2021).
19. Sureyya Rifaioglu, A., Dogan, T., Jesus Martin, M., Cetin-Atalay, R. & Atalay, V. DEEPred: Automated Protein Function Prediction with Multi-task Feed-forward Deep Neural Networks. *Sci Rep* **9**, 7344 (2019).
20. Dutta, P., Patra, A.P. & Saha, S. DeePROG: Deep Attention-Based Model for Diseased Gene Prognosis by Fusing Multi-Omics Data. *IEEE/ACM Trans Comput Biol Bioinform* **19**, 2770-2781 (2022).
21. Byeon, H. et al. Deep neural network model for enhancing disease prediction using auto encoder based broad learning. *SLAS Technol* **29**, 100145 (2024).

22. Gao, L. et al. Identifying noncoding risk variants using disease-relevant gene regulatory networks. *Nat Commun* **9**, 702 (2018).
23. Kelley, D.R. et al. Sequential regulatory activity prediction across chromosomes with convolutional neural networks. *Genome Res* **28**, 739-750 (2018).
24. Alipanahi, B., Delong, A., Weirauch, M.T. & Frey, B.J. Predicting the sequence specificities of DNA- and RNA-binding proteins by deep learning. *Nat Biotechnol* **33**, 831-838 (2015).
25. Zhou, J. & Troyanskaya, O.G. Predicting effects of noncoding variants with deep learning-based sequence model. *Nat Methods* **12**, 931-934 (2015).
26. Zaheer, M. et al. Big bird: Transformers for longer sequences. *Advances in neural information processing systems* **33**, 17283-17297 (2020).
27. Ji, Y., Zhou, Z., Liu, H. & Davuluri, R.V. DNABERT: pre-trained Bidirectional Encoder Representations from Transformers model for DNA-language in genome. *Bioinformatics* **37**, 2112-2120 (2021).
28. Mo, S. et al. Multi-modal self-supervised pre-training for regulatory genome across cell types. *arXiv preprint arXiv:2110.05231* (2021).
29. Trotter, M., Nguyen, C.Q., Young, S., Woodruff, R. & Branson, K. in ICLR 2023- Machine Learning for Drug Discovery workshop (
30. Zhou, Z. et al. in The Twelfth International Conference on Learning Representations (2024).
31. Nguyen, E. et al. Hyenadna: Long-range genomic sequence modeling at single nucleotide resolution. *Advances in neural information processing systems* **36** (2024).
32. Zhang, D. et al. DNAGPT: a generalized pretrained tool for multiple DNA sequence analysis tasks. *bioRxiv*, 2023.2007. 2011.548628 (2023).
33. Zhu, X. et al. CD-GPT: A Biological Foundation Model Bridging the Gap between Molecular Sequences Through Central Dogma. *bioRxiv*, 2024.2006. 2024.600337 (2024).
34. Cheng, J. et al. Accurate proteome-wide missense variant effect prediction with AlphaMissense. *Science* **381**, eadg7492 (2023).
35. Brandes, N., Goldman, G., Wang, C.H., Ye, C.J. & Ntranos, V. Genome-wide prediction of disease variant effects with a deep protein language model. *Nat Genet* **55**, 1512-1522 (2023).
36. Steinhaus, R., Robinson, P.N. & Seelow, D. FABIAN-variant: predicting the effects of DNA variants on transcription factor binding. *Nucleic Acids Res* **50**, W322-W329 (2022).
37. Consortium, E.P. An integrated encyclopedia of DNA elements in the human genome. *Nature* **489**, 57-74 (2012).
38. Sherry, S.T. et al. dbSNP: the NCBI database of genetic variation. *Nucleic Acids Res* **29**, 308-311 (2001).
39. Landrum, M.J. et al. ClinVar: improvements to accessing data. *Nucleic Acids Res* **48**, D835-D844 (2020).
40. Norollahi, S.E. et al. Practical immunomodulatory landscape of glioblastoma multiforme (GBM) therapy. *J Egypt Natl Canc Inst* **36**, 33 (2024).
41. Wu, W. et al. Glioblastoma multiforme (GBM): An overview of current therapies and mechanisms of resistance. *Pharmacol Res* **171**, 105780 (2021).
42. Anjum, K. et al. Corrigendum to "Current status and future therapeutic perspectives of glioblastoma multiforme (GBM) therapy: A review" [Biomed. Pharmacother. 92 (2017) 681-689]. *Biomed Pharmacother* **101**, 820 (2018).
43. Hanif, F., Muzaffar, K., Perveen, K., Malhi, S.M. & Simjee Sh, U. Glioblastoma Multiforme: A Review of its Epidemiology and Pathogenesis through Clinical Presentation and Treatment. *Asian Pac J Cancer Prev* **18**, 3-9 (2017).

44. Anjum, K. et al. Current status and future therapeutic perspectives of glioblastoma multiforme (GBM) therapy: A review. *Biomed Pharmacother* **92**, 681-689 (2017).
45. Liang, J. et al. Prognostic factors of patients with Gliomas - an analysis on 335 patients with Glioblastoma and other forms of Gliomas. *BMC Cancer* **20**, 35 (2020).
46. Delgado-Lopez, P.D. & Corrales-Garcia, E.M. Survival in glioblastoma: a review on the impact of treatment modalities. *Clin Transl Oncol* **18**, 1062-1071 (2016).
47. Hasner, M.C., van Opijnen, M.P., de Vos, F.Y.F., Cuppen, E. & Broekman, M.L.D. Whole genome sequencing in (recurrent) glioblastoma: challenges related to informed consent procedures and data sharing. *Acta Neurochir (Wien)* **166**, 266 (2024).
48. Wrzeszczynski, K.O. et al. Whole Genome Sequencing-Based Discovery of Structural Variants in Glioblastoma. *Methods Mol Biol* **1741**, 1-29 (2018).
49. Van Nostrand, E.L. et al. A large-scale binding and functional map of human RNA-binding proteins. *Nature* **583**, 711-719 (2020).
50. Tong, X., Gao, Y. & Su, Z. Interaction of CTCF and CTCFL in genome regulation through chromatin architecture during the spermatogenesis and carcinogenesis. *PeerJ* **12**, e18240 (2024).
51. Sobocinska, J. et al. Zinc Finger Proteins in Head and Neck Squamous Cell Carcinomas: ZNF540 May Serve as a Biomarker. *Curr Oncol* **29**, 9896-9915 (2022).
52. Forcella, P. et al. SAFB regulates hippocampal stem cell fate by targeting Drosha to destabilize Nfib mRNA. *Elife* **13** (2024).
53. Zhang, W. et al. Oncogenic and immunological values of RBM34 in osteosarcoma and its pan-cancer analysis. *Am J Cancer Res* **13**, 5094-5121 (2023).
54. Fang, J. et al. TAF15 inhibits p53 nucleus translocation and promotes HCC cell 5-FU resistance via post-transcriptional regulation of UBE2N. *J Physiol Biochem* (2024).
55. Bhave, S.A. et al. Human SMAD4 Genomic Variants Identified in Individuals with Heritable and Early-Onset Thoracic Aortic Disease. *Cardiogenetics* **11**, 132-138 (2021).
56. Pozzetti, L., East, M.P., Laitinen, T. & Asquith, C.R.M. TLK2: a target for cancer and viral latency. *Nat Rev Drug Discov* **23**, 886 (2024).
57. Wang, Z. et al. AMPKalpha1-mediated ZDHHC8 phosphorylation promotes the palmitoylation of SLC7A11 to facilitate ferroptosis resistance in glioblastoma. *Cancer Lett* **584**, 216619 (2024).
58. Toton, E. et al. Impact of PKCepsilon downregulation on autophagy in glioblastoma cells. *BMC Cancer* **18**, 185 (2018).
59. Kenchappa, R.S. et al. Protein kinase C(iota) and SRC signaling define reciprocally related subgroups of glioblastoma with distinct therapeutic vulnerabilities. *Cell Rep* **37**, 110054 (2021).
60. Uht, R.M., Amos, S., Martin, P.M., Riggan, A.E. & Hussaini, I.M. The protein kinase C-eta isoform induces proliferation in glioblastoma cell lines through an ERK/Elk-1 pathway. *Oncogene* **26**, 2885-2893 (2007).
61. Chiba, A. et al. Midnolin, a Genetic Risk Factor for Parkinson's Disease, Promotes Neurite Outgrowth Accompanied by Early Growth Response 1 Activation in PC12 Cells. *Mol Cell Biol* **44**, 516-527 (2024).
62. Pangeni, R.P. et al. Genome-wide methylomic and transcriptomic analyses identify subtype-specific epigenetic signatures commonly dysregulated in glioma stem cells and glioblastoma. *Epigenetics* **13**, 432-448 (2018).
63. Murnyák, B. et al. PARP1 expression and its correlation with survival is tumour molecular subtype dependent in glioblastoma. *Oncotarget* **8**, 46348 (2017).
64. Bisht, P., Kumar, V.U., Pandey, R., Velayutham, R. & Kumar, N. Role of PARP Inhibitors in Glioblastoma and Perceiving Challenges as Well as Strategies for Successful Clinical Development. *Front Pharmacol* **13**, 939570 (2022).

65. Zaman, S., Chobrutskiy, B.I., Sikaria, D. & Blanck, G. MAPT (Tau) expression is a biomarker for an increased rate of survival for low-grade glioma. *Oncol Rep* **41**, 1359-1366 (2019).
66. Callari, M. et al. Cancer-specific association between Tau (MAPT) and cellular pathways, clinical outcome, and drug response. *Sci Data* **10**, 637 (2023).
67. Chen, J., Chen, Q., Wu, C. & Jin, Y. Genetic variants of the C11orf30-LRRC32 region are associated with childhood asthma in the Chinese population. *Allergol Immunopathol (Madr)* **48**, 390-394 (2020).
68. Han, Z., Jia, J., Lv, Y., Wang, R. & Cao, K. Transcriptional expression of ZICs as an independent indicator of survival in gliomas. *Scientific Reports* **11**, 17532 (2021).
69. An, H. et al. ALS-linked FUS mutations confer loss and gain of function in the nucleus by promoting excessive formation of dysfunctional paraspeckles. *Acta Neuropathol Commun* **7**, 7 (2019).
70. Mirsof, D. et al. Mutations in NONO lead to syndromic intellectual disability and inhibitory synaptic defects. *Nat Neurosci* **18**, 1731-1736 (2015).
71. Pugacheva, E.M. et al. BORIS/CTCF epigenetically reprograms clustered CTCF binding sites into alternative transcriptional start sites. *Genome Biol* **25**, 40 (2024).
72. Debaugny, R.E. & Skok, J.A. CTCF and CTCFL in cancer. *Curr Opin Genet Dev* **61**, 44-52 (2020).
73. Wang, L. et al. Kaiso (ZBTB33) Downregulation by Mirna-181a Inhibits Cell Proliferation, Invasion, and the Epithelial-Mesenchymal Transition in Glioma Cells. *Cell Physiol Biochem* **48**, 947-958 (2018).
74. Kashiwagi, K. et al. Mutation of the SWI/SNF complex component Smarce1 decreases nucleosome stability in embryonic stem cells and impairs differentiation. *J Cell Sci* **137** (2024).
75. Yan, T. et al. ZNF384 transcriptionally activated MGST1 to confer TMZ resistance of glioma cells by negatively regulating ferroptosis. *Cancer Chemother Pharmacol* **94**, 323-336 (2024).
76. Li, A., Guo, Y., Yin, Z., Liu, X. & Xie, G. MTA2 is one of 14 Transcription factors predicting recurrence free survival in gastric cancer and promotes cancer progression by targeting MCM5. *J Cancer* **14**, 262-274 (2023).
77. Fu, W., Hou, X., Dong, L. & Hou, W. Roles of STAT3 in the pathogenesis and treatment of glioblastoma. *Front Cell Dev Biol* **11**, 1098482 (2023).
78. Zhang, C., Yang, M., Li, Y., Tang, S. & Sun, X. FOXA1 is upregulated in glioma and promotes proliferation as well as cell cycle through regulation of cyclin D1 expression. *Cancer Manag Res* **10**, 3283-3293 (2018).
79. Rodon, L. et al. Active CREB1 promotes a malignant TGFbeta2 autocrine loop in glioblastoma. *Cancer Discov* **4**, 1230-1241 (2014).
80. Feng, C. et al. Regulatory factor X1 is a new tumor suppressive transcription factor that acts via direct downregulation of CD44 in glioblastoma. *Neuro Oncol* **16**, 1078-1085 (2014).
81. Heinz, S. et al. Simple combinations of lineage-determining transcription factors prime cis-regulatory elements required for macrophage and B cell identities. *Mol Cell* **38**, 576-589 (2010).
82. Grant, C.E., Bailey, T.L. & Noble, W.S. FIMO: scanning for occurrences of a given motif. *Bioinformatics* **27**, 1017-1018 (2011).
83. Quinlan, A.R. & Hall, I.M. BEDTools: a flexible suite of utilities for comparing genomic features. *Bioinformatics* **26**, 841-842 (2010).

84. Jensen, M.A., Ferretti, V., Grossman, R.L. & Staudt, L.M. The NCI Genomic Data Commons as an engine for precision medicine. *Blood, The Journal of the American Society of Hematology* **130**, 453-459 (2017).
85. Benton, M.C. et al. Variant Call Format-Diagnostic Annotation and Reporting Tool: A Customizable Analysis Pipeline for Identification of Clinically Relevant Genetic Variants in Next-Generation Sequencing Data. *J Mol Diagn* **21**, 951-960 (2019).
86. Jones, D. et al. cgpCaVEManWrapper: Simple Execution of CaVEMan in Order to Detect Somatic Single Nucleotide Variants in NGS Data. *Curr Protoc Bioinformatics* **56**, 15 10 11-15 10 18 (2016).
87. Ye, K., Schulz, M.H., Long, Q., Apweiler, R. & Ning, Z. Pindel: a pattern growth approach to detect break points of large deletions and medium sized insertions from paired-end short reads. *Bioinformatics* **25**, 2865-2871 (2009).
88. Harrow, J. et al. GENCODE: the reference human genome annotation for The ENCODE Project. *Genome research* **22**, 1760-1774 (2012).